

THE APPLICATION OF WAVELET ANALYSIS TO EXTRACT PARTICLE SIZE INFORMATION FROM PARTICLE-LADEN FLOW IMAGES

Andrew OOI¹ and Julio SORIA²

¹Dept Mechanical & Manufacturing Engineering, University of Melbourne, Parkville, VIC 3052, AUSTRALIA

²CSIRO Division of Building Construction & Engineering, PO Box 56, Highett, VIC 3190, AUSTRALIA

ABSTRACT

A method to extract particle images of a desired particles size from a particle-laden flow image is introduced. The technique uses the two-dimensional wavelet transform to extract only those structures in the image which correspond to a given spatial scale, while preserving the spatial location of these structures in the image. Although the discrete Fourier transform is used in the computation of the wavelet transform, the technique is different to spatial Fourier filtering. The method has been applied to idealised images formed by Gaussian intensity distributions with different spatial scales. The analysing wavelet used in the illustration of this new method is a two-dimensional variation of the Mexican hat wavelet. The generation of images containing only particle images of a desired size using the Mexican hat wavelet analysis is demonstrated. The sensitivity characteristics of this wavelet are discussed.

NOTATION

a	scaling parameter
b	wavelet transform domain variable
D	effective diameter of ideal particle image
$g(x)$	analysing wavelet
$G(\alpha)$	Fourier transform of $g(x)$
$(P_{max})_a$	maximum possible value of the wavelet transform
$s(x)$	intensity distribution of idealised particle
$S(\alpha)$	Fourier transform of $s(x)$
$T(b, a)$	wavelet transform
x	spatial domain variable
α	frequency domain variable
σ	standard deviation of Gaussian particle image

INTRODUCTION

Particle-laden flows are important in many industrial processes, e.g. the dispersion of coal particles by turbulence in furnaces. The fluid dynamics of particle-laden flows (or two-phase flows) is considerably more complex than single phase flows, and is a subject which has only recently been studied rigorously. Consideration of particle-laden flows has mainly been hindered by our lack of knowledge of single phase turbulent flows which are difficult to quantify in a general form. In addition, it has also been very difficult to measure important variables in particle-laden flows. Only recent advances in optical

technology and in the development of optical measuring techniques have made the measurement of pertinent quantities of both phases in turbulent particle-laden flows possible.

The interaction of particles with wall bounded turbulent flows has been considered by Rashidi, *et al.* (1990). Young and Hanratty (1991) have studied the turbulent motion of solid particles in pipe flow with water. Prototypic flows for mixing are free shear flows which result from the mixing of two streams (laminar or turbulent) of unequal velocities. Fundamental examples of these flows are jets, mixing layers and wakes. These flows are characterised by large scale structures which grow and pair during their evolution. Crowe *et al.* (1988) and Lazaro and Lasheras (1992a) have investigated the particle dispersion characteristics in developing mixing layers, while Lazaro and Lasheras (1992b) have investigated the particle dispersion in forced mixing layers. The structure of particle-laden round jets has been studied by Longmire and Eaton (1991) and Call and Kennedy (1991).

Most of these investigations have used optical flow imaging techniques. The reasons for using optical techniques as the preferred measurement methods for experimental investigations of particle-laden flows are obvious. Some of the primary variables in these studies are size and velocity of the particles. Neuman and Umhauer (1991) have developed a technique based on pulsed-laser holography to measure size and velocity of low concentration flows. As with most holographic methods the set-up is complex. Kim and Lee (1990) used a pattern recognition technique peculiar to circles in combination with a photographic method to measure the size of spherical spray drops.

The technique described here can be used with images of particles, as exemplified in Fig 1. This image was acquired with a high resolution CCD camera (1280 x 1024 pixel) which was double exposed using laser illumination. Thus in principle, it should be possible to determine the velocity distributions of the particles. Some of the desirable data to be extracted from this type of image are the association of particle sizes with respective particle velocities at a given spatial positions in the flow. In general, particles of different sizes have different velocities in the same spatial region of the flow. This results in great difficulties in the measurement of the velocity of the particles.

One method which allows the determination of the

spatial velocity distribution of particles of a desired size is to generate a sub-image of the original image which only contains particle images of the desired particle size. In principle, this can be done for a range of particle sizes, yielding the spatial velocity distributions for this given particle size range. It is the generation of these sub-images which was the primary motivation for the development of the method illustrated in this paper.

Wavelets are a tool for time-frequency localisation, and as such wavelet transforms have been used to extract frequency contents locally in time (Daubechies, 1992). An analog of this principle can be applied to extract space-scale information in two-dimensional physical space. Images of particles in a flow can be thought of as localised structures of a given scale (i.e. size) in the image (i.e. space). Since the desired result is to extract a given scale in some localised spatial position, it is proposed to use wavelets.

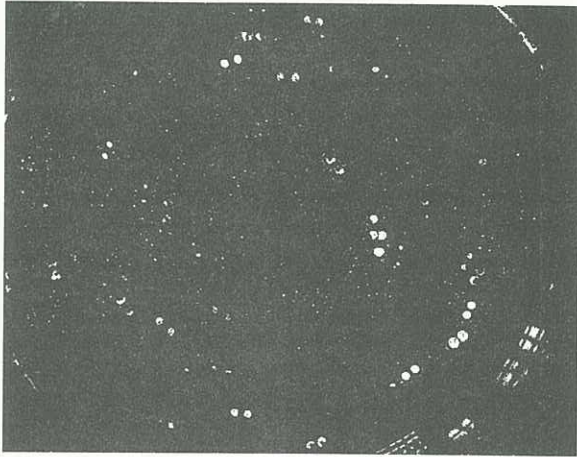


Fig 1 Image of particle-laden swirling flow showing a typical range of particle sizes.

THE CONTINUOUS WAVELET TRANSFORM

In two-dimensions, the wavelet transform $T(\mathbf{b}, a)$ is defined by the expression

$$T(\mathbf{b}, a) = \frac{1}{a} \int_{-\infty}^{\infty} \bar{g}\left(\frac{\mathbf{x} - \mathbf{b}}{a}\right) s(\mathbf{x}) d\mathbf{x} \quad (1)$$

where $g(\mathbf{x})$ is the wavelet function and $s(\mathbf{x})$ is the signal to be analysed. The overbar denotes the complex conjugate of $g(\mathbf{x})$. The scaling parameter a is defined for $a > 0$, and scales the analysing wavelet. The wavelet is squeezed (contracted) in the spatial domain for values of $a < 1$, while values of $a > 1$ expands it. Vector \mathbf{b} shifts the analysing wavelet through the domain. Thus, the wavelet transform can be regarded as a convolution between the analysing wavelet $g(\mathbf{x})$ and the signal $s(\mathbf{x})$ computed for different values of the scaling parameter a . Almost any function can be a wavelet, provided it satisfies the admissibility condition (Farge, 1990)

$$\int_{-\infty}^{\infty} |G(\alpha)|^2 \frac{d^2\alpha}{|\alpha|^2} < \infty \quad (2)$$

$G(\alpha)$ is the Fourier Transform of $g(\mathbf{x})$. Equation (2) actually implies that the wavelet has zero mean, i.e.

$$G(0) = 0.0 \quad (3)$$

In general, $g(\mathbf{x})$ is complex and thus $T(\mathbf{b}, a)$ may also be complex. In terms of its Fourier transform, the wavelet transform can also be written as (Smith, 1991)

$$T(\mathbf{b}, a) = \frac{a}{4\pi^2} \int_{-\infty}^{\infty} \bar{G}(a\alpha) S(\alpha) e^{i\mathbf{b}\cdot\alpha} d\alpha \quad (4)$$

Thus, the wavelet transform can be computed by sampling $\frac{1}{a} \bar{g}\left(\frac{\mathbf{x}}{a}\right)$ in physical space and then transforming to spectral space using the Fast Fourier Transform. The necessary convolution operation are performed more efficiently as Fourier space multiplications.

The following is a summary of the basic properties of the wavelet transform:

1. The wavelet transform contains no information about the mean value of the signal. This property is obvious from eq (4) together with the admissibility condition.
2. The wavelet transform is linear hence, the principle of superposition applies.
3. Shifting the signal in the spatial domain shifts the wavelet transform by the same amount.

$$\begin{aligned} s(\mathbf{x}) &\Leftrightarrow T(\mathbf{b}, a) \\ s(\mathbf{x} - \mathbf{X}_0) &\Leftrightarrow T(\mathbf{b} - \mathbf{X}_0, a) \end{aligned} \quad (5)$$

In the analysis that follows, properties (2) and (3) are used extensively.

APPLICATION OF WAVELET ANALYSIS TO AN IDEALISED SINGLE-PARTICLE IMAGE

The wavelet analysis of a single particle image is now considered. The formulae derived here can easily be applied to images with multiple particle images of different sizes by making use of the linearity property of the wavelet transform. The intensity distribution of a particle in the flow field is assumed to be Gaussian. The intensity of the Gaussian distribution decays to approximately 0.01 of its peak value at 3σ from the peak location, where σ is the standard deviation of the Gaussian. Hence, the effective diameter of the particle, D , is assumed to be 6σ .

In this illustration of the application of wavelet analysis, the two-dimensional Mexican hat wavelet has been chosen as the analysing wavelet due to the similarity of its shape to the idealised particle image. Note, that this wavelet might not be the optimum choice, and perhaps wavelets such as the "Gaussian Chirp" might prove to be a better choice. The equations defining the idealised particle image and the Mexican hat analysing wavelet (Fig 2) are respectively

$$s(x_1, x_2) = e^{-\frac{x_1^2 + x_2^2}{2\sigma^2}} \quad (6)$$

$$g(x_1, x_2) = (2 - (x_1^2 + x_2^2)) e^{-\frac{x_1^2 + x_2^2}{2\sigma^2}} \quad (7)$$

The wavelet transform of the ideal particle image using the Mexican hat wavelet is found to be

$$T(b_1, b_2, a) = \frac{a^3 \sigma^2 2\pi}{(a^2 + \sigma^2)^2} e^{-\frac{b_1^2 + b_2^2}{2(a^2 + \sigma^2)}} \left(2 - \frac{b_1^2 + b_2^2}{\sigma^2 + a^2}\right) \quad (8)$$

It is convenient to normalise the wavelet transform by the peak value computed for the matching scaling

factor a . It is easily shown that the peak value of the wavelet transform and the normalised wavelet transform are given by

$$(P_{max})_a = \pi a \quad (9)$$

$$T_{normalised}(b_1, b_2, a) = \frac{2(\frac{\sigma}{a})^2}{((\frac{\sigma}{a})^2 + 1)^2} e^{-\frac{b_1^2 + b_2^2}{2(\sigma^2 + a^2)}} (2 - \frac{b_1^2 + b_2^2}{\sigma^2 + a^2}) \quad (10)$$

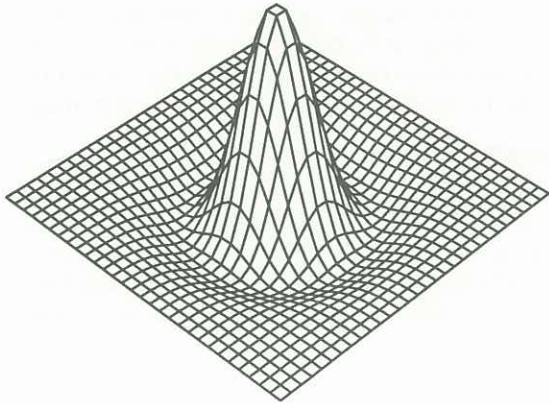


Fig 2 Functional distribution of the two-dimensional Mexican hat wavelet.

The normalised wavelet transform has some very interesting properties which are used to highlight particles of a desired size. To this end, the following properties of the normalised wavelet transform of a single idealised particle image have been deduced:

1. The normalised wavelet transform has a shape similar to the Mexican hat wavelet. Consideration of the normalised wavelet transform shows that it is nearly identical to the expression for the Mexican hat wavelet. The only differences being that its amplitude is dependent on the ratio σ/a and that it has been scaled by the factor $(\sigma^2 + a^2)$.
2. The peak of the normalised wavelet transform coincides with the location of the peak intensity of the particle. This property shows that the normalised wavelet transform can in fact detect the spatial location of particle images. More importantly, this property is independent of a and σ .
3. The maximum value of the normalised wavelet transform is 1.0 and occurs when $\sigma = a$. When this condition is satisfied, the scaling factor, a , scales the wavelet such that it best matches the size of the particle. Hence, if the condition $\sigma = a$ is not satisfied, then the peak of the normalised wavelet transform is less than unity and the particle image size is smaller or larger than the desired size.

The sensitivity of the normalised wavelet transform in detecting particles depends on the decay rate of the peak value of the normalised wavelet transform as a function of the ratio σ/a . Fig 3 is a graph of this sensitivity curve showing the decay rate of the peak value of the normalised wavelet transform as a function of σ/a . Note

that the curve is not symmetric. The shape of this curve is a function of the analysing wavelet and of the image shape, the effect of neither is considered here.

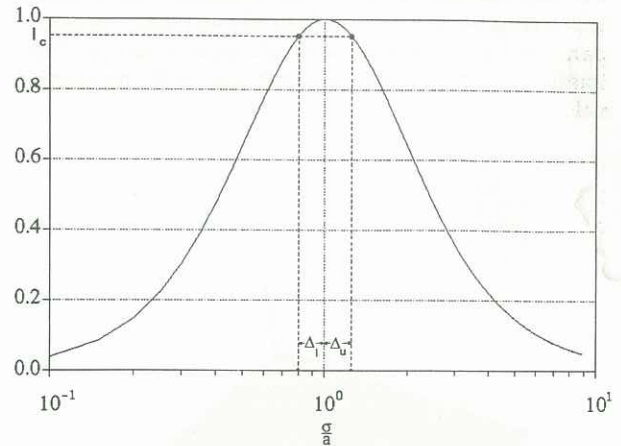


Fig 3 Sensitivity curve for two-dimensional Mexican hat wavelet.

The sensitivity curve provides a convenient basis on which to discriminate the particle size of particle images. Hence, if the size of the particle is within $(1 + \Delta_u)$ and $(1 - \Delta_l)$, its peak value will be greater than I_c , where I_c is the cut-off value resulting from the admissible size range $\Delta\sigma = a(\Delta_u + \Delta_l)$. Δ_u and Δ_l are as defined in Fig 3.

PARTICLE DETECTION FROM AN IDEALISED MULTI-PARTICLE IMAGE

Using the basic properties of the wavelet transform and the properties of the normalised wavelet transform for a single particle, an image containing 4 ideal particle images of different sizes is considered. Fig 4 shows the intensity distribution of the image. The image contains particles with effective diameters $D/3$, D and $4D$, where $D = 6\sigma_i$ and σ_i is the standard deviation of the Gaussian intensity distribution.

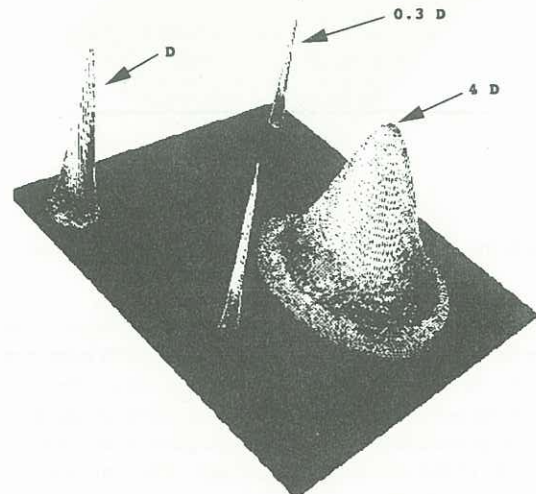


Fig 4 Intensity distribution of multi-particle idealised image.

Fig 5 shows the wavelet transform of the idealised image computed with $a = \sigma_i/3$, i.e. this transform should select the smallest particles. Note that the wavelet transform has been divided by $(P_{max})_a$ (eq 9). Fig 6 shows the

wavelet transform with $a = 4\sigma_i$, this wavelet transform should select the largest particles. Note that only the positive part of the normalised wavelet transforms is used as it is only this part of the wavelet transform that is useful in detecting particles in the desired size range. As can be seen from Figs 5 and 6 these transformed images predominantly contain information of particles with the selected size.

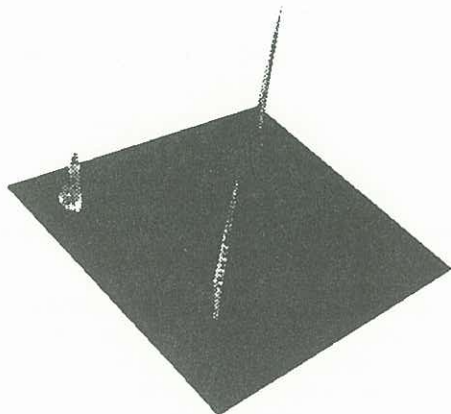


Fig 5 Intensity distribution of wavelet transformed image detecting particles of 0.3D.

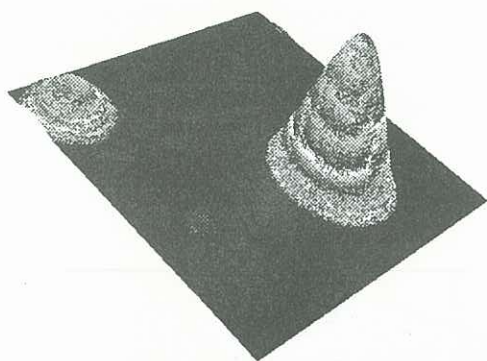


Fig 6 Intensity distribution of wavelet transformed image detecting particles of 4.0D.

The effect of proximity of two particle images of different size on their wavelet transform has also been considered. If the particle images are too close, then the peak of the wavelet transform of the particle image to be detected is reduced by the negative part of the wavelet transform of the other particle image. This can result in detection problems.

CONCLUSIONS

The applicability of the principle of using the normalised wavelet transform to detect particles of a desired size from a two-dimensional multi-particle image has been demonstrated. The wavelet transform can be

used to synthesise sub-images containing only particles of a desired size. Care has to be exercised if particle images are too close together, as this can result in detection problems. A detailed analysis of this effect has yet to be undertaken.

The technique described in this paper is relatively easy to apply to a digitised version of an image containing particles in a flow. The deduction of the size of particles and their location does not involve the direct measurement of the diameter of the particles. Only the position of the local peak values of the normalised wavelet transform are required to determine the size of the particle images and their location. It remains for this method to be tested on real particle images, e.g. Fig 1. Note that additional angular scaling can be included in the wavelet transform which can extend the applicability of the wavelet transform to the detection of "non-circular" particle images.

ACKNOWLEDGMENTS

The work presented here was undertaken while A. Ooi was a Vacation Scholar at the CSIRO Division of Building, Construction and Engineering. Support from the Mechanical and Manufacturing Engineering Department at the University of Melbourne is also acknowledged.

REFERENCES

- CALL, C.J. and KENNEDY, I.M. (1991) A technique for measuring Lagrangian and Eulerian particle statistics in a turbulent flow. *Exp Fluids*, **12**, 125-130.
- CROWE, C.T., CHUNG, J.N. and TROUTT, T.R. (1988) Particle mixing in free shear flows. *Prog. Energy Combust Sci*, **14**, 171-194.
- DAUBECHIES, I. (1992) Ten lectures on wavelets. SIAM.
- FARGE M, GUEZENNEC Y, HO C.M. and MENEVEAU C (1990) Continuous wavelet analysis of coherent structures. Stanford University, Center for Turbulence Research, Proceedings of the Summer Program, 331-348
- KIM, I.G. and LEE, S.Y. (1990) A simple technique for sizing and counting spray drops using digital image processing. *Exp Thermal Fluid Sci*, **3**, 214-221.
- LAZARO, B.J. and LASHERAS, J.C. (1992a) Particle dispersion in a developing free shear layer. Part 1. Unforced flow. *J Fluid Mech*, **235**, 143-178.
- LAZARO, B.J. and LASHERAS, J.C. (1992b) Particle dispersion in a developing free shear layer. Part 2. Forced flow. *J Fluid Mech*, **235**, 179-221.
- LONGMIRE, E.K. and EATON, J.K. (1992) Structure of a particle-laden round jet. *J Fluid Mech*, **236**, 217-257.
- NEUMANN, P. and UMHAUER, H. (1991) Characterization of the spatial distribution state of particles transported by a turbulent gas flow. *Exp Fluids*, **12**, 81-89.
- RASHIDI, M., HETSRONI, G. and BANERJEE, S. (1990) Particle-turbulence interaction in a boundary layer. *Int J Multiphase Flow*, **16**, 935-949.
- SMITH R.W., PODDAR K. and SMITS A.J. (1991) Application of the wavelet transform to the analysis of turbulent flows. (Submitted for publication)
- YOUNG, J.B. and HANRATTY, T.J. (1991) Optical studies on the turbulent motion of solid particles in a pipe flow. *J Fluid Mech*, **231**, 665-688.